

Regulation of Vascular Smooth Muscle Tone by N-terminal Region of Caldesmon

POSSIBLE ROLE OF TETHERING ACTIN TO MYOSIN*

(Received for publication, October 26, 1999)

Young-Ho Lee‡, Cynthia Gallant‡, HongQui Guo§, Yanhua Li§, C.-L. Albert Wang§, and Kathleen G. Morgan‡||

From the ‡Signal Transduction Group and the §Muscle Research Group, Boston Biomedical Research Institute, Boston, Massachusetts 02114 and the ¶Cardiovascular Division, Beth Israel Deaconess Medical Center and Harvard Medical School, Boston, Massachusetts 02215

To assess the functional significance of tethering actin to myosin by caldesmon in the regulation of smooth muscle contraction, we investigated the effects of synthetic peptides, containing the myosin-binding sequences in the N-terminal region of caldesmon, on force directly recorded from single permeabilized smooth muscle cells of ferret portal vein. Two peptides were used, IK29C and MY27C, containing residues from Ile²⁵ to Lys⁵³ and from Met¹ to Tyr²⁷ of the human and chicken caldesmon sequence, respectively, plus an added cysteine at the C terminus. In cells clamped at pCa 6.7, both peptides increased basal tone. Pretreatment of cells at pCa 6.7 with IK29C or MY27C decreased the amplitude of subsequent phenylephrine-induced contractions but not microcystin-racemic mixture-induced contractions. In all cases the effects of the peptides were concentration-dependent, and IK29C was more potent than MY27C, in agreement with their relative affinity toward myosin. The peptides were ineffective after the phenylephrine contraction was established. MY27C did not further increase the magnitude of contraction caused by a maximally effective concentration of IK29C, consistent with the two peptides having the same mechanism of action. Neither polylysine nor two control peptides containing scrambled sequences of IK29C, which do not bind myosin, had any effect on basal or phenylephrine-induced force. Our results suggest that IK29C and MY27C induce contraction by competing with the myosin-binding domain of endogenous caldesmon. Digital imaging of fluoroisothiocyanate-tagged IK29C confirmed the association of the peptide with intracellular filamentous structures. The results are consistent with a model whereby tethering of actin to myosin by caldesmon may play a role in regulating vascular tone by positioning the C-terminal domain of caldesmon so that it is capable of blocking the actomyosin interaction.

Phosphorylation of Ser¹⁹ of the 20-kDa myosin light chain (LC₂₀)¹ by Ca²⁺-calmodulin-dependent myosin light chain kinase (MLCK) has clearly been shown to represent a major

pathway for the regulation of contractile force in vascular smooth muscle (1–2). However, regulation by LC₂₀ phosphorylation may not explain all aspects of smooth muscle contractility. In particular, with respect to tonic contractile responses, many examples of dissociation between force levels, LC₂₀ phosphorylation levels, intracellular Ca²⁺ concentration ([Ca²⁺]_i), and cross-bridge cycling rates have been reported (2–5), and the possible existence of a secondary regulatory mechanism for smooth muscle contraction is difficult to negate. Although the precise mechanism involved in this additional regulatory system has not yet been identified, one likely candidate for mediating this regulation is the thin filament-associated protein caldesmon.

Smooth muscle caldesmon consists of three parts (Fig. 1), N-terminal, C-terminal, and an elongated central spacer region (6–7). The C-terminal portion of the molecule contains binding sites for actin and tropomyosin and inhibits actin-activated ATPase activity of myosin *in vitro* (8–15). Both N- and C-terminal fragments include binding sites for calmodulin (16–17). The N-terminal portion of the molecule also contains a binding site for myosin that may be involved in tethering actin to myosin (18).

Evidence that caldesmon is involved in the regulation of contraction has been reported from several groups using different approaches. We have previously reported the effect of a peptide, GS17C, that contains residues from Gly⁶⁵¹ to Ser⁶⁶⁷ of the C-terminal caldesmon sequence. The peptide binds actin but does not inhibit actomyosin ATPase activity and when used in saponin-permeabilized single ferret aortic and portal vein cells produced a sustained contraction (19). It was postulated that the contraction was due to competition with and partial displacement of endogenous caldesmon, resulting in disinhibition of myosin ATPase activity (19). It has been reported that extraction of caldesmon from a permeabilized smooth muscle preparation increased the Ca²⁺ sensitivity of force development (20) and, conversely, that addition of caldesmon or a C-terminal fragment to permeabilized chicken gizzard fibers inhibited contraction (21–22). It has also been reported recently that, in arterial strips made caldesmon-deficient by the use of antisense oligodeoxynucleotides, increased basal cross-bridge cycling rates are inhibited by the addition of caldesmon (23).

Most investigations into the possible role of caldesmon in smooth muscle contractility have focused on the role of the

* This work was supported by KOSEF (to Y.-H. L.), Grant AR41637 (to C.-L. A. W.) and Grants HL31704 and HL42293 (to K. G. M.).

|| To whom correspondence and reprint requests should be addressed: Boston Biomedical Research Inst., 20 Staniford St., Boston, MA 02114, Tel.: 617-912-0331; Fax: 617-227-6053; E-mail: morgan@bbri.org.

¹ The abbreviations used are: LC₂₀, 20-kDa myosin light chain; MLCK, myosin light chain kinase; PE, phenylephrine; MOPS, 4-morpholinepropanesulfonic acid; HBSS, Hank's balanced salt solution;

[Ca²⁺]_i, intracellular Ca²⁺ concentration; MAPK, mitogen-activated protein kinase; FITC, fluorescence isothiocyanate; Fmoc, N-(9-fluorenyl)methoxycarbonyl; HMM, heavy meromyosin; microcystin-LR, microcystin racemic mixture.

C-terminal part of caldesmon. However, because caldesmon contains both actin (C-terminal) and myosin (N-terminal) binding domains, both have been postulated to play a role in force maintenance in smooth muscle through a tethering effect that may maintain contractile force in the absence of cross-bridge cycling (24). As an alternative hypothesis, tethering has also been postulated to function as in a structural manner, keeping the contractile filaments in register (25). However, at the present time, direct evidence is still lacking for a role of the N-terminal part of caldesmon in the contraction of smooth muscle cells.

Thus, we synthesized a 29-residue peptide, IK29C,² and a 27-residue peptide, MY27C (26–27), which contain residues from Ile²⁵ to Lys⁵³ and from Met¹ to Tyr²⁷, derived from the myosin-binding domain of human and chicken caldesmon sequence, respectively, with an added cysteine at the C terminus. Both peptides have been shown to bind to smooth muscle myosin, but IK29C binds more strongly than does MY27C.² To test the hypothesis that tethering of caldesmon may function as a physiological regulator of vascular tone, we determined the effects of IK29C, MY27C, and related peptides on contractility in a single hyperpermeable cell system (28–29). Our results strongly suggest that IK29C and MY27C induce contraction by competing with the myosin-binding domain of endogenous caldesmon and, furthermore, that tethering of caldesmon may play a role in regulating vascular tone by properly positioning the C terminus of caldesmon so that it can maximally inhibit the actin-activated myosin ATPase.

EXPERIMENTAL PROCEDURES

Peptides and Drugs—All peptides were synthesized as amides on an automated peptide synthesizer (ABI-431A) on a 0.25-mmol scale using the “FastMoc” method (30), a procedure similar to the Fmoc protocol except the activation is performed with 2-(1*H*-benzotriazol-1-yl)-1,3,3-tetramethyluronium hexafluorophosphate, instead of by carbodiimide-mediated reactions. 1.2 g of Rink (4-(2',4'-dimethoxyphenyl)-Fmoc-aminomethyl)-phenoxy resin (Advanced ChemTech, Louisville, KY) was used for each synthesis. After synthesis the peptides were cleaved from the resin according to a trifluoroacetic acid-based protocol in a solution containing 0.75 g of phenol, 0.25 ml of 1,2-ethanedithiol, 0.5 ml of thioanisole, 10.0 ml of trifluoroacetic acid, and 1.0 ml of H₂O at room temperature. To ensure complete removal of the protecting group (2,2,5,7,8-pentamethyl-chroman-6-sulfonyl chloride) for Arg residues, the reaction time was increased to 4 h for IK29C and its variants. After cleavage/deprotection reaction the peptide was precipitated upon dropwise addition of the reaction mixture into cold diethyl ether. The peptide was then spun down, washed by ether, dialyzed against water, and lyophilized.

The peptides were first examined by reversed phase high pressure liquid chromatography using an analytical C-8 column (Si-O-Si-(CH₂)₇-CH₃ from Phenomenex, Torrance, CA; length, 250 mm; internal diameter, 4.6 mm; particle size, 5 mm). About 100 μ l of 2 mg/ml of peptide solution (in water) was injected each time, and the column was eluted with a 0–60% acetonitrile gradient containing 0.1% trifluoroacetic acid at a flow rate of 1 ml/min. The peptides were eluted with increasing concentrations of Solution B (100% acetonitrile plus 0.1% trifluoroacetic acid). The peptides were then purified using a semi-preparative C-8 column (length, 250 mm; internal diameter, 10 mm; particle size, 5 mm) with an injection volume of 500 μ l (of 2 mg/ml) and a flow rate of 2 ml/min. The bulk of each peak was collected, dialyzed against water, and lyophilized. All peptides thus purified were confirmed by both amino acid composition and partial sequence analyses and were further checked by MALDI-TOF mass spectrometry (Perspective Biosystems, Voyager RP) to ascertain the purity and complete removal of protecting groups. In each case a single major peak was obtained; their respective masses (*m/z*) were 3817.72 (IK29C), 3815.96 (IK29CX1), 3814.79 (IK29CX2), and 3765.95 (MY27C).

The following drugs were used: PE, creatine kinase, phosphocreatine, and microcystin-LR (all from Sigma). General laboratory reagents were of analytical grade or better and were purchased from Sigma or Fisher.

Solutions—Ca²⁺ buffers were prepared according to an iterative computer program that calculates the amounts of stock solutions required for a given set of free ion concentrations, taking into consideration the binding constants for the ionic species present, temperature, and ionic strength (28). Ionic strength was set at 0.2 M, and MOPS was used to buffer the pH at 7.0. The concentrations of the constituents were as follows: Ca²⁺, 1 nM TO 0.1 mM; Mg²⁺, 1 mM; K⁺, 135 mM; MgATP, 3 mM; EGTA, 15 mM; MOPS, >15 mM; phosphocreatine, 15 mM; and creatine kinase (approximately 20 units/ml), added daily before the experiments. The major anion was propionate. Krebs solution (used only for dissection of the tissue) contained (in mM) 120 NaCl, 5.9 KCl, 2.5 CaCl₂, 1.2 MgCl₂, 25 NaHCO₃, 1.2 NaH₂PO₄, and 11.5 dextrose at pH 7.4 when bubbled with 95% O₂ + 5% CO₂. The Ca²⁺-Mg²⁺-free Hank's balanced salt solution (HBSS) used for cell isolation contained (in mM) 137 NaCl, 5.4 KCl, 0.44 KH₂PO₄, 4.17 NaHCO₃, 0.42 NaH₂PO₄, and 5.5 dextrose, 10 HEPES, pH 7.4.

Tissue Preparation and Single Cell Isolation—All procedures were performed according to protocols approved by the Institutional Animal Care and Use Committee. Ferrets were euthanized with chloroform, and the portal vein was quickly removed to a dissection dish filled with oxygenated Krebs solution. The tissue was cleaned of connective tissue and opened longitudinally, and the endothelium was removed by gentle abrasion of the inner surface of the tissue with a rubber policeman. The tissue was cut into 2–3-mm-wide strips, and wet weight was determined. Single vascular smooth muscle cells from ferret portal vein were isolated using a modification of a previously published method (29). The portal vein was cut into small pieces (2 × 2 mm) and placed in a siliconized flask containing digestion medium. For each 50 mg of portal vein (wet weight), the digestion medium A consisted of 4.2 mg of CLS 2 collagenase (type II, 228 units/mg; Worthington) and 4 mg of elastase (Grade II, 3.65 units/mg; Roche Molecular Biochemicals) in 7.5 ml of Ca²⁺-Mg²⁺-free HBSS and 1% bovine serum albumin (Life Technologies, Inc.). The tissue pieces were incubated in a shaking water bath at 34 °C under an atmosphere of 95% O₂ + 5% CO₂ for 45 min. The pieces were then filtered on a nylon mesh, rinsed with 10 ml of Ca²⁺-Mg²⁺-free HBSS, and reincubated for 20 min in digestion medium B, i.e. the same digestion solution except for a decrease in the amount of collagenase to 2.1 mg and addition of 5,000 units of soybean trypsin inhibitor (type II-S; Sigma). The tissue pieces were filtered and rinsed in 10 ml of Ca²⁺-Mg²⁺-free HBSS. The filtrate containing the dissociated cells was poured over unsiliconized glass coverslips and further incubated for 20 min in digestion medium B. After filtering and rinsing with 10 ml of Ca²⁺-Mg²⁺-free HBSS, the dissociated cells were plated onto another set of coverslips. Coverslips were stored on ice for 1–5 h until use. Cells were not centrifuged or aspirated by pipette. The isolated cells were assayed daily to confirm that they shortened in response to 10^{−5} M PE in 2.5 mM Ca²⁺-HBSS.

Permeabilization and Tension Measurement—The coverslips were placed on the movable stage of a Nikon inverted microscope. Ferret portal vein cells were exposed to a relaxing solution (pCa 9) containing 30 μ g/ml saponin for 5 min, and then the solution was changed to saponin-free pCa 6.7 solution. Permeabilized cells were chosen according to the following criteria: diminished phaselucence under phase-contrast optics; a visible nucleus; length \geq 100 μ m; and firm attachment to the coverslip. We have previously found that our permeabilization method results in cells that retain receptor-coupled function (29) and does not cause a detectable loss of molecules such as calmodulin (28). Microtools (Glass 1, Life Technologies, Inc., W/FIL 1.0 mm, 1B100F-4, 12773–08H, World Precision Instruments, Sarasota, FL) were prepared by the use of a micropipette puller (Industrial Science Associates, Inc. Ridgewood, NY), and the diameters of the tip of the microtool were < 5 μ m. The microtools were placed with their tips touching the top surface of the cell (microtools approached the coverslip at an angle of approximately 45°), and the cells were left undisturbed for 2–3 min. We have found that mammalian vascular smooth muscle cells prepared in this manner have the important advantage of sticking to glass and, therefore, readily attach to the glass microelectrodes. The microtool attached to the transducer (Cambridge model 400A) was lifted so that the end of the cell was raised off the coverslip. The other microtool was gently pressed down to immobilize the other end of the cell, which was stretched to approximately 110% of its original length. Control recordings confirmed the drift of the transducer was negligible over the course of the recording. At least one recording was made daily with a cell attached to the microtool in the absence of added drugs to

² Y. Li, S. Zhuang, K. Mabuchi, R. C. Lu, and C.-L. Albert Wang, unpublished results. Co-sedimentation experiments showed that both MY27C and IK29C bind smooth muscle myosin. The scrambled peptides, IK29CX1 and IK29CX2, however, did not appreciably co-sediment with myosin.

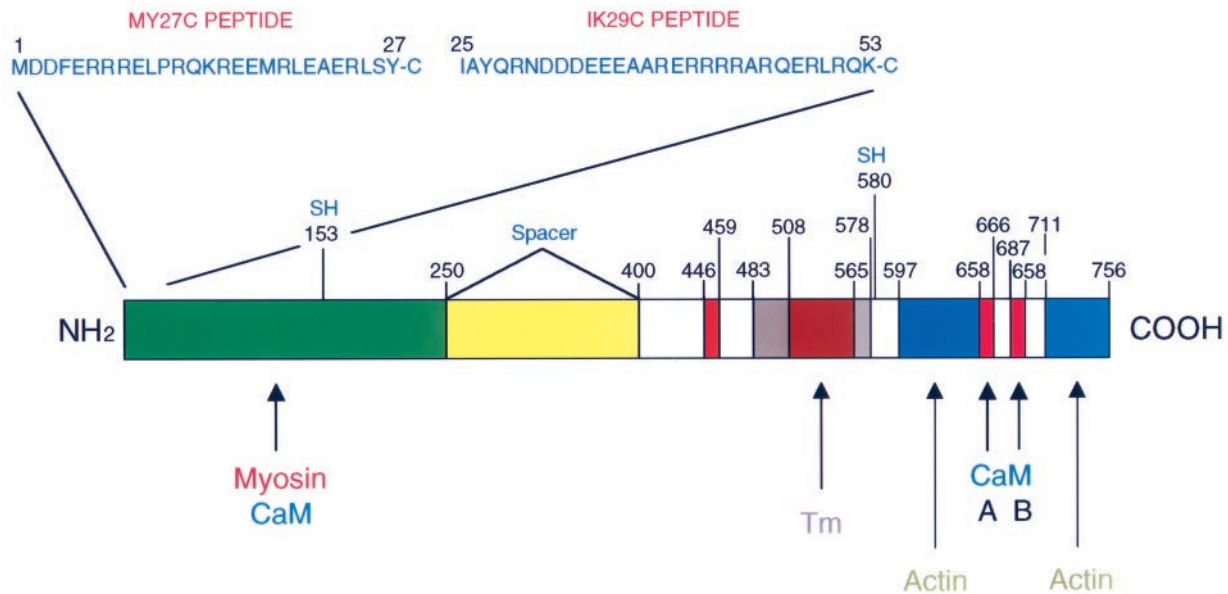
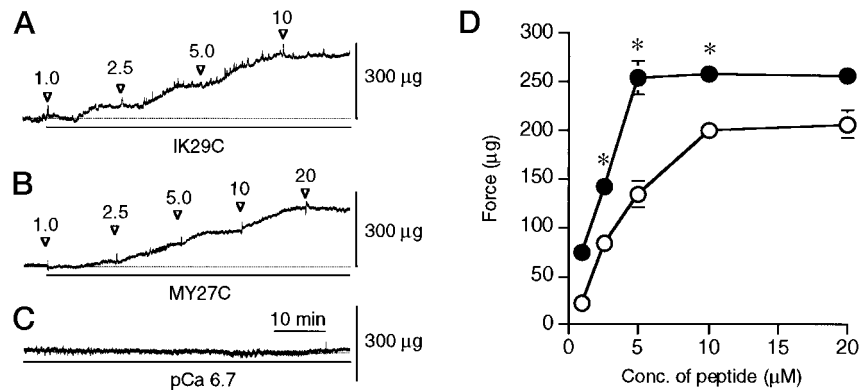


FIG. 1. **Domain structure of caldesmon.** The numbering of the complete caldesmon sequence corresponds to that of chicken gizzard isoform. The positions of IK29C (from Ile²⁵ to Lys⁵³ from the human sequence) and MY27C (Met¹ to Tyr²⁷ from the chicken sequence) are also shown.

FIG. 2. **Effects of IK29C or MY27C on basal tension.** In all panels, tension was recorded from single permeabilized portal vein cells at *p*Ca 6.7. **A**, concentration dependence of IK29C-induced increases in basal tension. **B**, concentration dependence of MY27C-induced increases in basal tension. **C**, control trace. Dotted line indicates basal force at *p*Ca 6.7. Concentrations (μ M) of IK29C and MY27C, respectively, are shown. **D**, statistical analysis of the effects of IK29C and MY27C on basal tension; *, $p < 0.05$ compared with contraction induced by MY27C.



confirm that the base line drifted $\leq 10 \mu\text{g}$ over the time course of an experiment. Additionally, base-line recordings of 3–5 min were obtained for each cell before experimental manipulations were performed. Agonist-induced increases or decreases in force were assumed to have reached a plateau when no further increase or decrease occurred over a 2–3-min period. Force records were quantitated by placing a ruler on the trace through the midpoint of the noise level. All experiments were performed at 20–21 °C.

Digital Imaging—Isolated portal vein cells were incubated in *p*Ca 6.7 solution containing FITC-labeled IK29C peptide (5 μM) and saponin (30 $\mu\text{g}/\text{ml}$) for 10 min. The cells were then rinsed with *p*Ca 6.7 solution several times, fixed with 4% paraformaldehyde, and mounted with Fluoromount (Calbiochem) before analysis. Images were obtained using a Nikon Diaphot 300 inverted microscope equipped with a Nikon X-40 oil immersion objective (NA 1.3). Filters used were $470 \pm 20 \text{ nm}$ (excitation), 505 nm (dichroic), and $535 \pm 20 \text{ nm}$ (emission) for FITC-labeled cells. Images were recorded with a liquid cooled charge-coupled device (CCD) camera (photometrics CH250) via Photometrics Microsoft-compatible Image-processing Software (PMISTM).

For the comparison of LC₂₀ phosphorylation levels, cells were co-stained with a monoclonal (mouse) antibody (1:500) specific for phosphorylation of LC₂₀ at the MLCK sites, which was a gift from Drs. Y. Sasaki and M. Seto (Asahi Chemical Industry Co., Fuji, Japan) and has been previously characterized (31) and with rhodamine phalloidin (1:2000, Molecular Probes) to label actin. For data analysis, a region was identified containing a filament bundle, and fluorescence for both LC₂₀ phosphorylation and actin were quantitated and integrated, and the ratio of LC₂₀ phosphorylation fluorescence/actin fluorescence was calculated. Normalization of phosphorylation values by the actin content compensated for any differences in cell thickness, etc., between cells. The anti-phospho-LC₂₀ signal was visualized with an Oregon Green-

labeled goat anti-mouse secondary antibody (1:500, Molecular Probes). The Oregon Green signal was excited at $485 \pm 5.2 \text{ nm}$, and emission was measured through a dichroic filter at $>500 \text{ nm}$ and an emission filter at $515 \pm 4 \text{ nm}$. The rhodamine signal was excited at $546 \pm 12 \text{ nm}$, and emission was measured through a dichroic filter at $>580 \text{ nm}$ and a barrier filter at $>590 \text{ nm}$. Cells labeled only with Oregon Green were viewed with the rhodamine filter set, and cells labeled only with rhodamine were viewed with the Oregon Green filter set to confirm that there was no significant cross-talk between channels at the gain settings used.

Myosin and Actomyosin ATPase Activity Assays—Both unphosphorylated and phosphorylated recombinant gizzard HMM (expressed in insect cells from a clone kindly given by Dr. M. Ikebe) were used. For myosin phosphorylation, to purified HMM (0.97 mg/ml) in 50 mM NaCl, 20 mM Tris, pH 7.5, 1 mM dithiothreitol were added: 50 μl of recombinant rabbit smooth muscle MLCK (6.36 μM ; a gift from Dr. Z. Grabarek), 1.2 μl of calmodulin (267 μM), 5.25 μl of ATP (0.2 M, pH 7.4), 0.2 μl of CaCl_2 (1 M), 1.05 μl of MgCl_2 (1 M), at room temperature; total volume 1 ml; the mixture was incubated for 2 h and stored on ice. Immediately before the ATPase assay, phosphorylated HMM was passed through a gel filtration column at room temperature to remove ATP. ATPase was assayed by a continuous spectrophotometric method using 2-amino-6-mercapto-7-methylpurine ribonucleoside/purine nucleoside phosphorylase reaction to detect the released inorganic phosphate (EnzChek Kit from Molecular Probes, Eugene, OR) (32). Reaction conditions are as follows: 30 mM NaCl, 10 mM HEPES, pH 7.5, 5 mM MgCl_2 , 0.2 mM CaCl_2 , 0.5 mM ATP, 25 °C; 10–30 $\mu\text{g}/\text{ml}$ phosphorylated or unphosphorylated HMM, 4 μM actin, 0.57 μM tropomyosin; total volume = 0.5 ml.

Statistics—All values given in the text are mean \pm S.E. Differences between mean were evaluated using Student's *t* test. Significant differ-

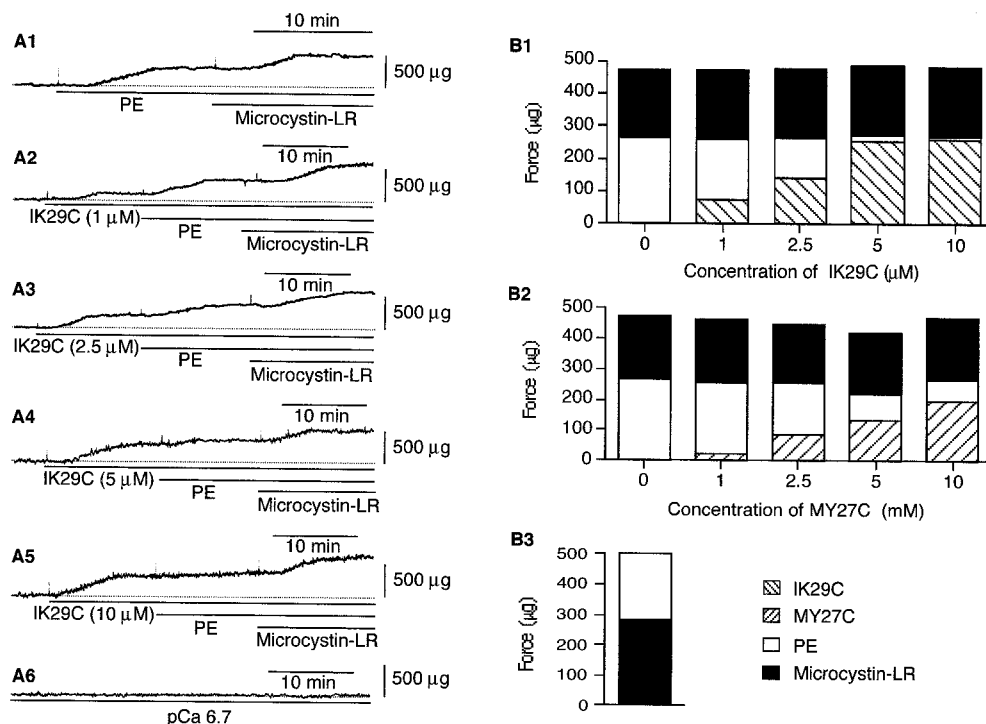
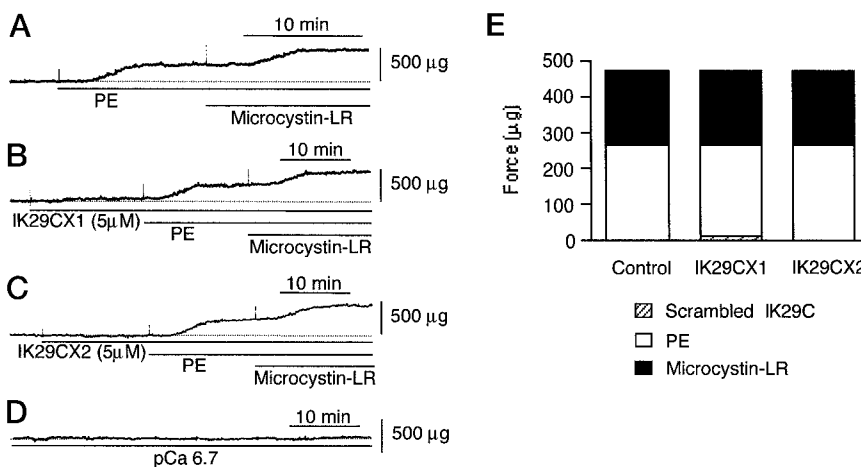


FIG. 3. Effects of pretreatment with IK29C or MY27C on PE- or microcystin-LR-induced contraction. A1, effects of PE (10^{-5} M) and subsequent addition of microcystin-LR (1 μ M) on single cell contractility. A2–A5, effects of pretreatment of the cells with IK29C on PE- or microcystin-LR-induced contractions. A6, control recording. Dotted line indicates base-line force at pCa 6.7. B1 and B2, average results of the effects of pretreatment with IK29C (B1) or MY27C (B2) on PE- and microcystin-LR-induced contraction ($n = 5$ –7). B3, average effect of 1 μ M microcystin-LR and subsequent addition of 10^{-5} M PE ($n = 5$).

FIG. 4. Effects of pretreatment with scrambled IK29C on PE- or microcystin-LR-induced contractions. A, force recording in response to PE (PE, 10^{-5} M) and microcystin-LR (1 μ M). B and C, effects of pretreatment of the cells with IK29CX1 (B) or IK29CX2 (C) on PE- or microcystin-LR-induced contraction. D, control recording. Dotted line indicates base-line force at pCa 6.7. E, average results of pretreatment with IK29CX1 ($n = 4$) or IK29CX2 ($n = 5$) on PE- and microcystin-LR-induced contraction.



ences were taken at the $p < 0.05$ level. The values given represent numbers of cells used in each experiment.

RESULTS

N-terminal Caldesmon Peptides Increase Resting Tension—Peptide IK29C contains 29 amino acid residues, IAYQRNDDEEEAARERRRRARQERLRQK, which correspond to the human caldesmon sequence from Ile²⁵ to Lys⁵³ (Fig. 1), plus a cysteine residue added at the C terminus. Peptide MY27C contains 27 amino acid residues, MDDFERRRELRRQKREEMRLEAERLSY, which corresponds to the chicken caldesmon sequence from Met¹ to Tyr²⁷ (Fig. 1), and a C-terminal cysteine residue. The effects of these peptides on resting tension of single permeabilized ferret portal vein cells are illustrated in Fig. 2. In cells in which Ca^{2+} was clamped at pCa 6.7, both peptides induced a gradual but sustained increase in contractile force (Fig. 2, A and B). The mean steady-state increase in force in response to IK29C was 74 ± 7.5 μ g ($n = 5$) at 1 μ M,

142 ± 6.1 μ g ($n = 6$) at 2.5 μ M, 254 ± 17.1 μ g ($n = 6$) at 5 μ M, 258 ± 11.4 μ g ($n = 5$) at 10 μ M, and 257 ± 10.6 μ g ($n = 5$) at 20 μ M. In the case of MY27C, the mean steady-state amplitude of contraction was 22 ± 9.7 μ g ($n = 5$) at 1 μ M, 83 ± 12 μ g ($n = 6$) at 2.5 μ M, 134 ± 14 μ g ($n = 5$) at 5 μ M, 200 ± 10.9 μ g ($n = 5$) at 10 μ M, and 206 ± 14.5 μ g ($n = 3$) at 20 μ M. In both cases, the peptide-induced contractions were concentration-dependent, but IK29C was more potent and more effective than MY27C. The maximal force developed by the peptides was 258 ± 11.4 μ g for IK29C and 206 ± 14.5 μ g for MY27C, respectively. The 50% effective concentrations (EC_{50}) of IK29C and MY27C were 1.98 and 3.4 μ M, respectively.

PE and Microcystin-LR Effects Are Additive—The effects of PE and microcystin-LR on the contractility of single permeabilized ferret portal vein cells are illustrated in Fig. 3. As shown in Fig. 3A1, a maximally effective concentration of PE (10^{-5} M) evoked a gradual but sustained contraction of permeabilized

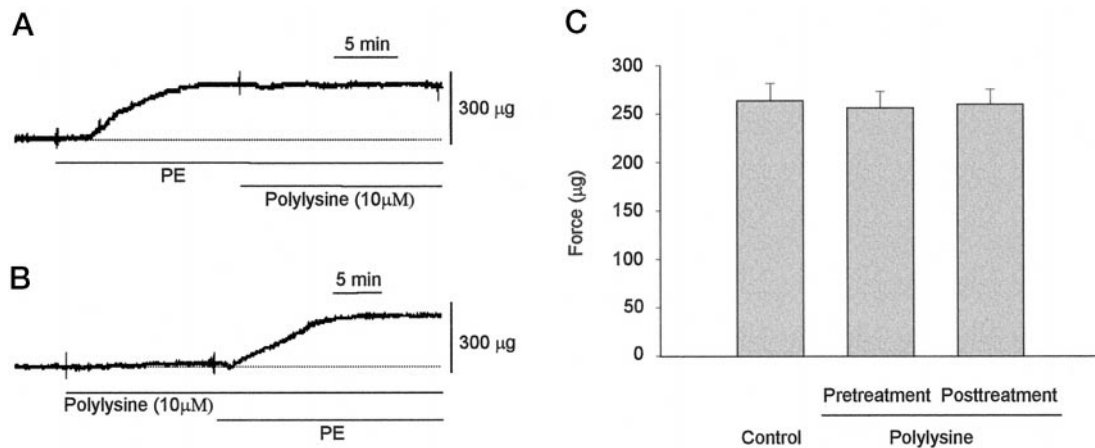


FIG. 5. **Effect of polylysine on basal and PE-induced contractions.** Polylysine was added to single permeabilized cells in *p*Ca 6.7 buffer either after treatment with PE in A or before PE treatment in B. Polylysine had no effect on basal tone. There was no significant effect of polylysine on PE-induced contractions in either the pretreatment or post-treatment protocol (C) ($n = 6$).

portal vein cells clamped at *p*Ca 6.7. The mean steady-state increase in force in response to PE was $266 \pm 20.2 \mu\text{g}$ ($n = 7$) (Fig. 3B1). When portal vein cells were stimulated by PE, the subsequent addition of microcystin-LR ($1 \mu\text{M}$) caused a further increase in force generation above that induced by PE (Fig. 3A1), and the mean steady-state increase was $206 \pm 27.2 \mu\text{g}$ ($n = 7$) (Fig. 3B1). We have previously shown that ferret portal vein and aortic cells contract in response to PE at near resting $[\text{Ca}^{2+}]_i$ levels in the absence of changes in LC_{20} phosphorylation, and this contraction is associated with activation of protein kinase C and mitogen-activated protein kinase (MAPK) and phosphorylation of the C-terminal half of caldesmon (29, 33–36). In contrast, it is known that microcystin-LR is an inhibitor of myosin light chain phosphatase that causes contraction by increasing LC_{20} phosphorylation levels (37). We have previously shown that microcystin-LR provokes a contraction in single permeabilized ferret cells independent of activation of protein kinase C (38). The additivity of the PE and microcystin-LR responses is consistent with their having different mechanisms of action.

It is of interest that when microcystin-LR was added first, it induced a larger contraction ($284 \pm 12.1 \mu\text{g}$, $n = 5$, Fig. 3B3, $p = 0.04$) than when microcystin-LR was added after PE contraction was established ($206 \pm 27.2 \mu\text{g}$, $n = 7$, Fig. 3B1). Similarly, post-treatment of cells with PE after the induction of a microcystin-LR contraction evoked an average, smaller contraction ($222 \pm 12 \mu\text{g}$, $n = 5$, Fig. 3B3, $p = 0.102$) than that caused by PE alone ($266 \pm 20.2 \mu\text{g}$, $n = 7$, Fig. 3B1), although the difference did not reach statistical significance. When the sum of the PE and microcystin-LR contractions was compared across the different protocols (Fig. 3B1, 2, and 3), it was noticed that the total force produced was remarkably similar, between 480 and 500 μg . Thus, it appears that there is a “ceiling” of about 500 μg on the total force that a single ferret portal vein cell can generate.

N-terminal Caldesmon Peptides Inhibit PE but Not Microcystin-LR Contractions—The effects of pretreatment of single permeabilized ferret portal vein cells with IK29C or MY27C on the PE- or microcystin-LR-induced contraction are illustrated in Fig. 3. Pretreatment of the cells with IK29C or MY27C decreased the amplitude of PE-induced contractions but not that of microcystin-LR-induced contractions. As shown in Fig. 3A, as the concentration of IK29C or MY27C increased, the effect on basal tension also increased but the amplitude of the subsequent PE-induced contraction decreased. In contrast, increasing concentrations of the peptides had no effect on the magnitude of the microcystin-LR-induced contraction. Fig. 3,

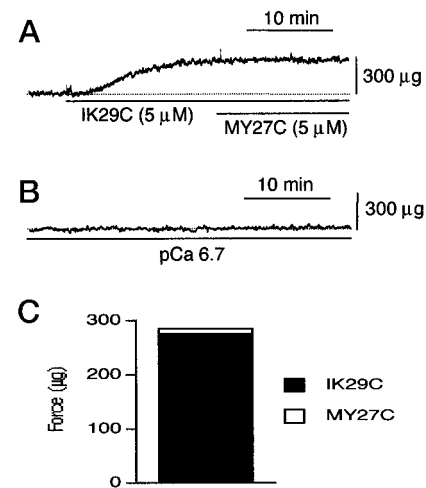
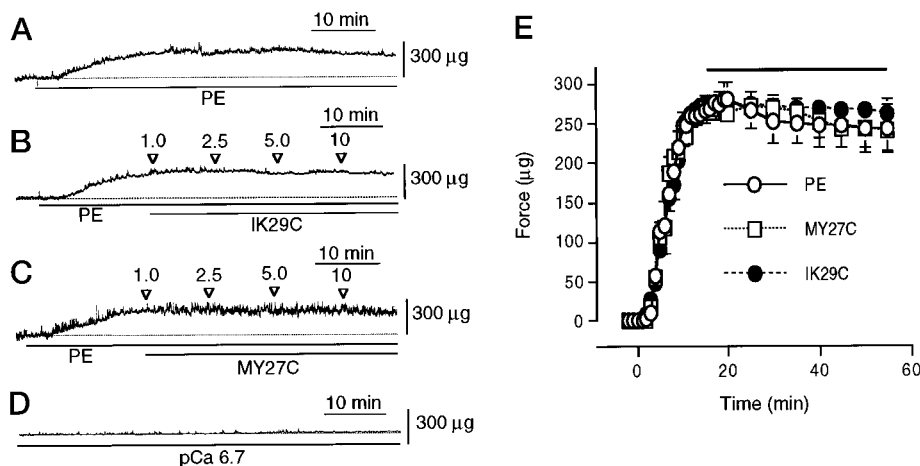


FIG. 6. **Effects of pretreatment of cells with IK29C on MY27C-induced contraction.** A, force recording in response to IK29C ($5 \mu\text{M}$) and subsequent addition of MY27C ($5 \mu\text{M}$). B, control recording. Dotted line indicates base-line force at *p*Ca 6.7. C, average response to pretreatment with IK29C, followed by MY27C ($n = 5$).

B1 and B2, show the sum of the mean peptide-, PE-, and microcystin-LR-induced contraction in the presence of various concentrations of the peptide. At $1 \mu\text{M}$ IK29C, the IK29C-induced contraction was $74 \pm 7.5 \mu\text{g}$ ($n = 5$), and the amplitude of PE- or microcystin-LR-induced contraction was $188 \pm 13.6 \mu\text{g}$ ($n = 5$) and $212 \pm 7.4 \mu\text{g}$ ($n = 5$), respectively. However, in $10 \mu\text{M}$ IK29C, the IK29C-induced contraction was increased to $258 \pm 11.4 \mu\text{g}$ ($n = 5$), and PE-induced contraction was decreased to $23 \pm 13.9 \mu\text{g}$ ($n = 5$), but microcystin-LR-induced contraction ($212 \pm 5.8 \mu\text{g}$, $n = 5$) was not altered. The inhibition of the PE-induced contraction by the peptides was concentration-dependent, and again, IK29C was more potent than MY27C.

Two different scrambled versions of IK29C, IK29CX1 (RE-AERARQREIDLRLAREKQ RAERYDQRND-C) and IK29CX2 (EEEEEDDDQQAALYQNRNRRRRRRARRRK-C), were synthesized and were tested for effects on contractility. $5 \mu\text{M}$ IK29CX1 or IK29CX2 produced little or no increase in resting tension (Fig. 4) and had no detectable effect on PE- or microcystin-LR-induced contractions. The amplitude of contraction in response to PE with or without IK29CX1 was $253 \pm 17 \mu\text{g}$ ($n = 4$) and $266 \pm 20.2 \mu\text{g}$ ($n = 7$), respectively. The amplitude of contraction in response to microcystin-LR with or without IK29CX1 was $208 \pm 12.5 \mu\text{g}$ ($n = 4$) and $206 \pm 27.2 \mu\text{g}$ ($n = 7$),

FIG. 7. Effects of post-treatment with IK29C or MY27C on PE-induced contraction. *A*, force recording in the presence of PE (10^{-5} M). *B*, effects of increasing concentration (μ M) of IK29C (arrows) on PE-induced contraction. *C*, effects of increasing concentration (μ M) of MY27C (arrows) on PE-induced contraction. *D*, control recording. Dotted line indicates base-line force at pCa 6.7. Solid line above PE, IK29C, or MY27C, exposure period to PE or peptide. *E*, average results on the effects of IK29C or MY27C on the PE-induced contraction ($n = 5$).



respectively. 5μ M IK29CX2 had similar results to IK29CX1. Although IK29CX2 was designed to retain the polyarginine motif of IK29C, since polylysine has been reported to activate smooth muscle in a phosphorylation-independent manner (39), we directly tested the effect of polylysine in our system. However, even at the maximally effective concentration of IK29C with respect to contraction, polylysine had no effect on (Fig. 5) basal or phenylephrine-induced force in either a post-treatment (Fig. 5A) or a pretreatment (Fig. 5B) protocol.

If IK29C and MY27C have the same mechanism of action, then their maximal effects should not be additive. Indeed, as shown in Fig. 6, MY27C (5μ M) did not further increase the magnitude of contraction caused by a maximally effective concentration of IK29C (5μ M).

N-terminal Caldesmon Peptides Are Ineffective after PE-induced Contraction Is Established—The effects of IK29C or MY27C added after the PE-induced response had reached steady state are illustrated in Fig. 7. As shown in Fig. 7, when portal vein cells were stimulated by a maximally effective concentration of PE (10^{-5} M), the subsequent addition of IK29C (Fig. 7, *B* and *E*) or MY27C (Fig. 7, *C* and *E*) had no obvious effect on PE-induced contractions. As shown in Fig. 7A, the interpretation of the results was complicated by the fact that, with time, the PE-induced contraction tended to decrease slightly. When average results (Fig. 7E, $n = 5$) were compared at the same time points, however, there were no significant differences with and without the peptides.

FITC-labeled IK29C Distributes Non-homogeneously in Cells—Since IK29C and MY27C were postulated to alter contractility by competing with caldesmon for its binding site on myosin, we performed digital imaging experiments using FITC-IK29C to confirm internalization and verify whether the peptide has an intracellular distribution consistent with association with myosin filaments. As shown in Fig. 8, fluorescence appeared in a non-homogeneous, punctate distribution, running in a filamentous pattern parallel to the long axis of the cell. The staining pattern does not prove, but is consistent with, the distribution of FITC-labeled peptide along the bundles of contractile filaments in this cell type (40). The fact that the peptide was internalized in the core of the cell was confirmed by optical sectioning of the cell images.

IK29C Does Not Alter LC_{20} Phosphorylation in Cells—It is possible that the increase in force caused by IK29C could be due to an unknown effect of the peptide to increase phosphorylation of LC_{20} . For this reason, we assessed relative LC_{20} phosphorylation levels using an antibody specific for LC_{20} phosphorylated at the MLCK sites, as described under “Experimental Procedures.” Co-staining of actin with rhodamine phalloidin was used for normalization. As can be seen in Fig. 9, A

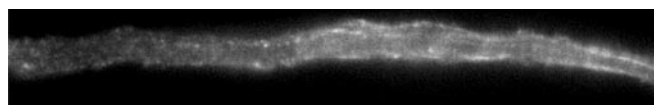


FIG. 8. Localization of IK29C. Resting portal vein cell showing localization of FITC-labeled IK29C. Cell diameter at widest point is $\sim 7 \mu$ m. See text for details.

and *B*, both stains characteristically labeled structures in similar filamentous bundles. The actin signal is expected to be constant except for changes in cell thickness at different pCa values. When the ratio of the phospho- LC_{20} signal to the actin signal was calculated (Fig. 9C), it was found to increase markedly between pCa 6.7 and 5.0 but not between pCa 6.7 and 6.7 plus peptide.

IK29C Does Not Directly Alter Actomyosin ATPase Activity—Another possibility is that the increase in force caused by IK29C is due to a direct effect to increase myosin ATPase activity in the absence of light chain phosphorylation. Thus, we determined the effect of 10μ M IK29C on myosin ATPase activity and on actin-activated myosin ATPase activity as described under “Experimental Procedures.” As is shown in Table I, although the addition of actin to unphosphorylated HMM caused a small increase in ATPase activity and the addition of actin to phosphorylated HMM caused a marked increase in ATPase activity, the addition of IK29C to unphosphorylated actomyosin caused no increase in ATPase activity.

DISCUSSION

The main purpose of the present study was to investigate a possible physiological role for N-terminal domain of caldesmon in the regulation of smooth muscle tone by using synthetic peptides based on N-terminal caldesmon sequences as experimental tools. It has been reported that caldesmon binds to smooth muscle myosin subfragment 2 (41) and that the binding site resides in the N-terminal region of caldesmon (25, 42). It has been reported that the major myosin-binding site is present between residues 24 and 53 of chicken gizzard smooth muscle caldesmon and that a second, weaker site may be present between residues 1 and 23 (25). It has also been reported by another group that two functionally different myosin-binding sites are located in residues 1–28 and 29–128 of chicken gizzard caldesmon (42). IK29C, a synthetic peptide corresponding to the human caldesmon sequence from Ile²⁵ to Lys⁵³, is found to bind strongly to smooth muscle myosin.² MY27C binds less strongly² and was less potent and less effective in the present study, consistent with the myosin binding domain of caldesmon being primarily located between residues 25 and 53, but also, to a lesser extent, extending to the N terminus.

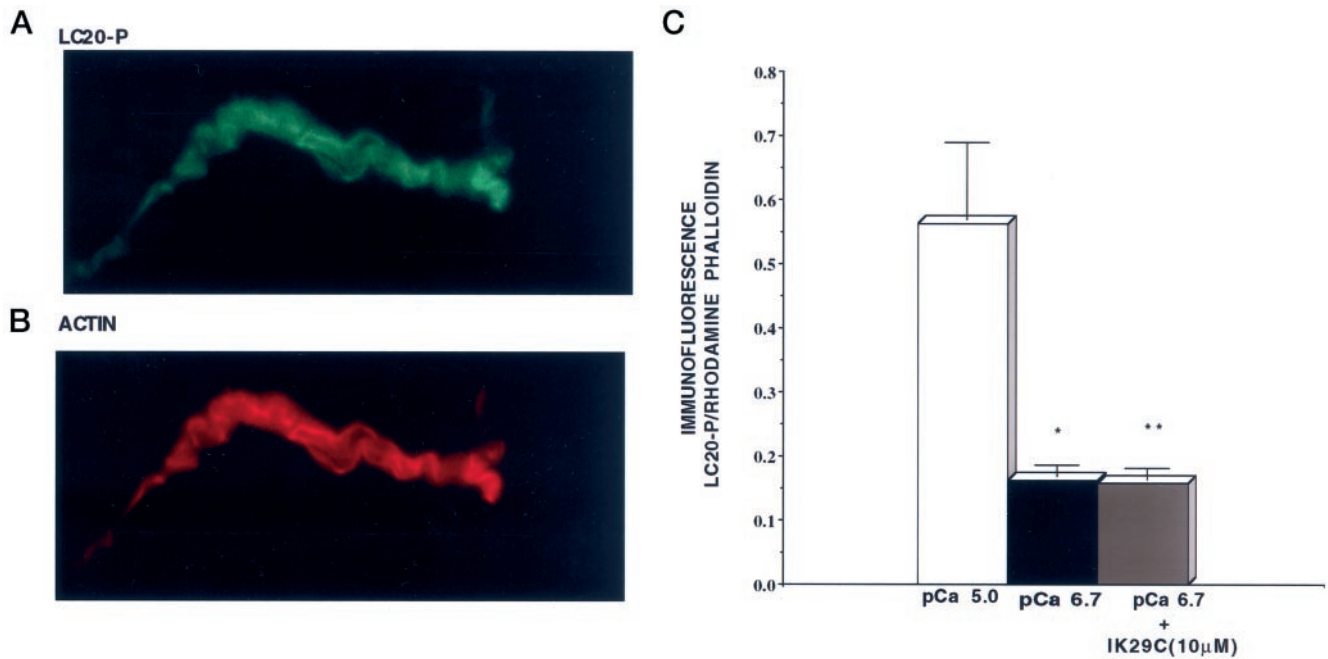


FIG. 9. Measurement of relative LC₂₀ phosphorylation levels. Cells were co-labeled with an antibody specific for LC₂₀ phosphorylated at the MLCK sites (A) and rhodamine phalloidin to label actin (B). For data analysis, a region containing a filament bundle was identified, and both LC₂₀ phosphorylation-induced fluorescence and actin-induced fluorescence were quantitated and integrated for the same region. The ratios of LC₂₀ phosphorylation to actin signals were compared in 9–13 cells in the presence of pCa 5, pCa 6.7 alone, or pCa 6.7 plus 10 μM IK29C (C).

TABLE I
Assay of *in vitro* myosin ATPase activity

Proteins	Rate
	$\mu\text{mol } P_i / \text{mg HMM} \cdot \text{min}$
pHMM + actin	0.171
pHMM alone	0.034
HMM alone	≤ 0.02
HMM + IK29C (10 μM)	0.022
HMM + actin	0.046
HMM + actin + IK29C (10 μM)	0.037

In the present study, we have introduced these peptides into single permeabilized portal vein cells to test the hypothesis that the binding of N-terminal caldesmon to myosin is important for the regulation of smooth muscle tone, either in the maintenance of force in the absence of cross-bridge cycling or as a structural protein, keeping the contractile proteins in proper register. We postulated that IK29C would displace endogenous caldesmon from myosin by binding the same site on myosin. Consistent with this hypothesis digital imaging studies confirmed that FITC-labeled IK29C introduced into cell binds discretely to structures that are organized in a filamentous pattern running down the long axis of the cell. We also found that IK29C, but not two scrambled peptides that do not bind myosin, induced a concentration-dependent increase in resting tone. These findings strongly suggest that the interference with N-terminal binding of caldesmon to myosin has a significant physiologic effect on vascular tone.

One of the control peptides used, IK29CX2, was designed to retain the polyarginine motif of IK29C, but because polylysine has been reported to contract smooth muscle in a phosphorylation-dependent manner, we also tested the effect of polylysine. However, none of these peptides had any detectable effect on force.

Since phosphorylation of LC₂₀ results in an increase in actin-activated myosin ATPase activity and an increased contractility, it was possible that IK29C might have nonspecific effects to either increase LC₂₀ phosphorylation or to increase directly

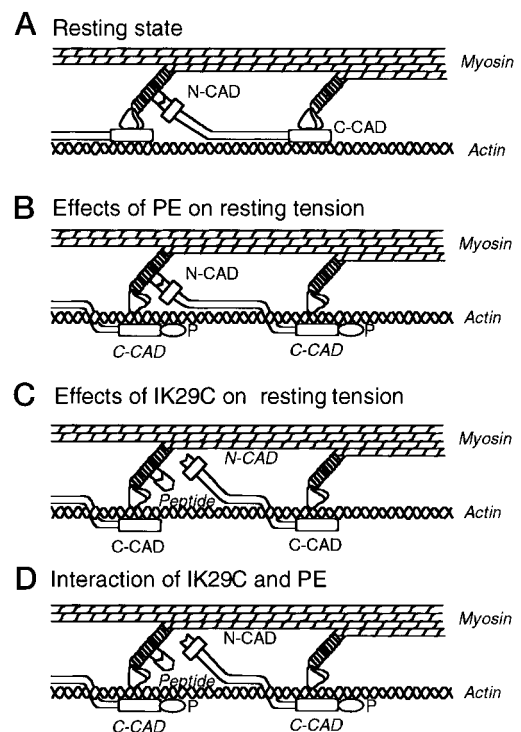


FIG. 10. Schematic representation of the possible mechanism of peptide- or PE-induced contraction. Phosphorylation is indicated by *P*. *Italics* indicated the activated (phosphorylated), in *C-CaD* or detached state from myosin molecule, in *N-CaD*. *N-CaD*, N-terminal of caldesmon; *C-CaD*, C-terminal of caldesmon. See text for details.

myosin ATPase activity. Thus, we compared phospho-LC₂₀ levels in individual cells with or without the peptide and *in vitro* myosin ATPase activity in the presence and absence of the peptide. We were unable to see any detectable effect of the peptide on phosphorylation or ATPase activity, consistent with an effect of the peptide specifically on interaction between the N-terminal segment of caldesmon and myosin.

Another major finding of the present study was that pretreatment of the cells with IK29C inhibited PE-induced contractions but not microcystin-LR-induced contractions. It has previously been reported that the α -adrenergic agonist, PE, elicits a contraction in ferret vascular smooth muscle cells, and this contraction is associated with phosphorylation of the C-terminal domain of caldesmon by activation of protein kinase C and MAPK (2, 35–36, 43). Conversely, microcystin-LR is known to be an inhibitor of myosin light chain phosphatase and to contract smooth muscle in the absence of changes in $[Ca^{2+}]_i$ by increasing LC₂₀ phosphorylation (37). Thus, in this system, at low $[Ca^{2+}]_i$ levels, PE is expected to cause contraction through thin filament regulation, whereas microcystin-LR is expected to cause contraction through thick filament regulation. In the present study, we found that PE and microcystin-LR responses are additive, consistent with their having different and independent mechanisms of action. The fact that the PE contraction but not the microcystin-LR contraction was affected by the (N-terminal) caldesmon peptides points to a specific disruption of thin filament regulation.

The fact that the increased contractile force caused by N-terminal caldesmon peptides and PE are not additive suggests a common, thin filament-based mechanism of action. However, as described above, the PE-induced contraction at constant $[Ca^{2+}]_i$ is thought to result in alleviation of the inhibitory effect of C-terminal caldesmon on actin-activated myosin ATPase activity, possibly by phosphorylation of the C-terminal of caldesmon by MAPK (35–36) (Fig. 10B). IK29C is derived from the N-terminal domain of caldesmon, which binds myosin, and, thus, one might expect addition of the peptide to break tethers and cause global relaxation of all contractions. This is not what was seen. Rather, a selective *prevention* of PE contractions but not microcystin contractions was seen. However, the results of the present study are consistent with a modified model illustrated in Fig. 10. As shown in Fig. 10C, our present study suggests that displacement of N terminus of caldesmon from myosin by IK29C may affect the “proper positioning” of the C terminus of caldesmon required for its inhibitory action on actin-activated myosin ATPase. Caldesmon displaced from this proper position would lead to disinhibition of actomyosin interaction and the resultant IK29C-induced contraction (Fig. 10C). This model is also consistent with a prevention of the PE-induced contraction in the presence of the peptide if they act through the same mechanism (Fig. 10D). We also found that post-treatment of the portal vein cells with IK29C had no effect on contraction induced by maximally effective concentration of PE. Thus, the peptide can prevent but not reverse the PE-induced contraction. It might be expected, if tethering of actin and myosin by caldesmon were involved in force maintenance, that the peptides would decrease force maintenance by breaking the tethers; however, if the C-terminal end of caldesmon is already disinhibited, the peptide would have no effect (Fig. 10D).

Although the results of the present study are consistent with the above model, we cannot rule out alternative interpretations, such as the possibility that the interaction of the N-terminal domain of CaD with myosin is inhibiting by constraining the position of the myosin head and that the CaD peptides relieve this constraint.

In conclusion, peptides from the myosin binding N-terminal region of caldesmon caused contraction of vascular smooth muscle cells and selectively prevented contraction by PE. These results are consistent with, but do not prove, the hypothesis

that tethering of N-terminal of caldesmon may play a role in regulating vascular tone by positioning the C terminus of caldesmon so that it is capable of inhibiting actin-activated myosin ATPase.

Acknowledgments—We thank Drs. Yasuharu Sasaki and Minoru Seto (Asahi Chemical Industry Company, Ltd., Shizuoka, Japan) for the gift of the anti-phospho-LC₂₀ monoclonal antibody, Dr. Mitsuo Ikebe (University of Massachusetts Medical Center, Worcester, MA) for the gift of recombinant gizzard HMM clone, and Dr. Zenon Grabarek (Boston Biomedical Research Institute, Boston, MA) for the gift of recombinant rabbit smooth muscle MLCK.

REFERENCES

- Kamm, K. E., and Stull, J. T. (1989) *Annu. Rev. Physiol.* **51**, 299–313
- Horowitz, A., Clément-Chomienne, O., Walsh, M. P., and Morgan, K. G. (1996) *Am. J. Physiol.* **271**, C589–C594
- Gerthoffer, W. T. (1987) *J. Pharmacol. Exp. Ther.* **240**, 8–15
- Moreland, S., Moreland, R. S., and Singer, H. A. (1987) *Pfluegers Arch.* **408**, 139–145
- Morgan, K. G., and Morgan, J. P. (1982) *Pfluegers Arch.* **395**, 75–77
- Bryan, J., Imai, M., Lee, R., Moore, P., Cook, R. G., and Lin, W.-G. (1989) *J. Biol. Chem.* **264**, 13873–13879
- Hayashi, K., Yamasada, S., Kanda, K., Kimizuka, F., Kato, I., and Sobue, K. (1989) *Biochem. Biophys. Res. Commun.* **161**, 38–45
- Bartegi, A., Fattoun, A., Derancourt, J., and Kassab, R. (1990) *J. Biol. Chem.* **265**, 15231–15238
- Collins, J. H., Leszyk, J., Mornet, D., and Audemard, E. (1991) *Protein Sequences & Data Anal.* **4**, 29–32
- Fujii, T., Imai, M., Rosenfeld, G. C., and Bryan, J. (1987) *J. Biol. Chem.* **262**, 2757–2763
- Hayashi, K., Fujio, Y., Kato, I., and Sobue, K. (1991) *J. Biol. Chem.* **266**, 355–361
- Marston, S. B., Moody, C. J., and Smith, C. W. J. (1984) *Biochem. Soc. Trans.* **12**, 945–948
- Ngai, P. K., and Walsh, M. P. (1984) *J. Biol. Chem.* **259**, 13656–13659
- Sobue, K., Morimoto, K., Inui, M., Kanda, K., and Kakiuchi, S. (1982) *Biomed. Res.* **3**, 188–196
- Wang, C.-L. A., Wang, L.-W. C., Xu, S., Lu, R. C., Saavedra-Alanis, V., and Bryan, J. (1991) *J. Biol. Chem.* **266**, 9166–9172
- Wang, C.-L. A., Wang, L.-W. C., Lu, R. C. (1989) *Biochem. Biophys. Res. Commun.* **162**, 746–752
- Wang, C.-L. A. (1988) *Biochem. Biophys. Res. Commun.* **156**, 1033–1038
- Velaz, L., Ingraham, R. H., and Chalovich, J. M. (1980) *J. Biol. Chem.* **265**, 2929–2934
- Katsuyama, H., Wang, C.-L. A., and Morgan, K. G. (1992) *J. Biol. Chem.* **267**, 14555–14558
- Malmqvist, U., Arner, A., Makuch, R., and Dabrowska, R. (1996) *Pfluegers Arch.* **432**, 241–247
- Szpacenko, A., Wagner, J., Dabrowska, R., and Ruegg, J. C. (1985) *FEBS Lett.* **192**, 9–12
- Pfitzer, G., Strauss, J. D., and Ruegg, J. C. (1992) *Jpn. J. Pharmacol.* **58**, 23–28
- Earley, J. J., Su, X., and Moreland, R. S. (1998) *Circ. Res.* **83**, 661–667
- Hemric, M. E., and Chalovich, J. M. (1988) *J. Biol. Chem.* **263**, 1878–1885
- Wang, Z., Jiang, H., Yang, Z. Q., and Chacko, S. (1997) *Proc. Natl. Acad. Sci. U. S. A.* **94**, 11898–11904
- Zhuang, S., and Wang, C.-L. A. (1997) *Mol. Biol. Cell* **8**, 156
- Zhuang, S., and Wang, C.-L. A. (1997) *Biophys. J.* **72**, 281
- Brozovich, F. V., Walsh, M. P., and Morgan, K. G. (1990) *Pfluegers Arch.* **416**, 742–749
- Collins, E. M., Walsh, M. P., and Morgan, K. G. (1992) *Am. J. Physiol.* **262**, H754–H762
- Wang, E., and Wang, C.-L. A. (1996) *Arch. Biochem. Biophys.* **329**, 156–162
- Sakurada, K., Seto, M., and Sasaki, Y. (1998) *Am. J. Physiol.* **274**, C1563–C1572
- Melki, R., Fievez, S., and Carlier, M.-F. (1996) *Biochemistry* **35**, 12038–12045
- Khalil, R. A., and Morgan, K. G. (1992) *J. Physiol. (Lond.)* **455**, 585–599
- Khalil, R. A., Lajoie, C., and Morgan, K. G. (1994) *Am. J. Physiol.* **266**, C1544–C1551
- Menice, C. B., Hulvershorn, J., Adam, L. P., Wang, C.-L. A., and Morgan, K. G. (1997) *J. Biol. Chem.* **272**, 25157–25161
- Dessy, C., Kim, I.-K., Sougniez, C. L., Laporte, R., and Morgan, K. G. (1998) *Am. J. Physiol.* **275**, C1081–C1086
- Gong, M. C., Cohen, P., Kitazawa, T., Ikebe, M., Masuo, M., Somlyo, A. P., and Somlyo, A. V. (1992) *J. Biol. Chem.* **267**, 14662–14668
- Katsuyama, H., and Morgan, K. G. (1993) *Circ. Res.* **72**, 651–657
- Szymanski, P. T., Strauss, J. D., Doerman, G., DiSalvo, J., and Paul, R. J. (1992) *Am. J. Physiol.* **262**, C1446–C1455
- Parker, C. A., Takahashi, K., Tang, J. X., Tao, T., and Morgan, K. G. (1998) *J. Physiol. (Lond.)* **508**, 187–198
- Ikebe, M., and Reardon, S. (1988) *J. Biol. Chem.* **263**, 3055–3058
- Vorotnikov, A. V., Marston, S. B., and Huber, P. A. J. (1997) *Biochem. J.* **328**, 211–218
- Walsh, M. P., Andrea, J. E., Allen, B. G., Clément-Chomienne, O., Collins, E. M., and Morgan, K. G. (1994) *Can. J. Physiol. Pharmacol.* **72**, 1392–1399

**Regulation of Vascular Smooth Muscle Tone by N-terminal Region of Caldesmon:
POSSIBLE ROLE OF TETHERING ACTIN TO MYOSIN**

Young-Ho Lee, Cynthia Gallant, HongQui Guo, Yanhua Li, C.-L. Albert Wang and
Kathleen G. Morgan

J. Biol. Chem. 2000, 275:3213-3220.
doi: 10.1074/jbc.275.5.3213

Access the most updated version of this article at <http://www.jbc.org/content/275/5/3213>

Alerts:

- [When this article is cited](#)
- [When a correction for this article is posted](#)

[Click here](#) to choose from all of JBC's e-mail alerts

This article cites 43 references, 17 of which can be accessed free at
<http://www.jbc.org/content/275/5/3213.full.html#ref-list-1>